International Journal of Engineering

Journal Homepage: www.ije.ir

Three Dimensional Modeling of Combustion Process and Emissions Formationin Pre and Main Chambers of an Idirect Injection Diesel Enginge

S. Jafarmadar*, R. Barzegar

Department of Mechanical Engineering, University of Urmia, Urmia, Iran,

PAPER INFO

Paper history:
Received 16 May 2012
Received in revised form 10 July 2012
Accepted 30 August 2012

Keywords:
Main and Pre Chambers
Indirect Injection
Emission
Performance
Three Dimensional Modeling

ABSTRACT

The combustion processes and emission formation in pre and main chambers of a Lister 8.1 IDI diesel are simulated with the Computational Fluid Dynamics (CFD) code. The model includes spray atomization, mixture formation and distribution and subsequently the combustion processes and emissions formation modeling are carried out with considering of flow configurations in two chambers. A part load (50% load) and a full load simulation of engine are carried out. Also, the amount of mass burning rate of fuel, temperature, heat losses and emissions formation in pre and main chamber are presented with more details. The simulation results, such as the mean in-cylinder pressure and exhaust emissions are compared with the measured values and show good agreement .This work demonstrates that multidimensional modeling can be used at complex chamber geometry to gain more insight into the flow field, combustion process and emissions formation. The simulation results show that the CFD combustion simulation tool works quite correctly for the predicting combustion process and emission formation in Lister 8.1 IDI diesel engine.

doi: *10.5829/idosi.ije.2012.25.04c.06*

1. INTRODUCTION

In a very competitive world improvement of engine performance has become an important issue for automotive manufacturers. In order to improve the engine performance, the combustion process and emission formation are now being studied in more detail. There are two common methods; experimental method and mathematical simulation (thermo-dynamical and CFD modeling) in engine research. Experimental methods obtain principal and valuable information, but are needed more costly equipment and time consumer.

Another approach for gaining insight into the in-cylinder flow is the application of three dimensional calculation codes, which are able to solve the governing flow equations, and thus yield detailed descriptions of the mean velocity and the turbulent velocity fields. Diesel engines are preferable to gasoline engines because of their high thermodynamic performance and low HC, CO and NOx emissions. HC and CO are lower because of more complete combustion of the fuel-air mixture. NOx is lower because the peak temperature is not maintained very long. The main emission in diesel engines is Soot, or smoke, that produces when there is insufficient air for complete combustion [1-4]. DI (direct injection) diesel engines are served ordinary as heavy duty engines and industrial usage, and IDI (indirect injection) diesel engines are used at automotive industries such as passenger cars. In an IDI diesel engine, the combustion chamber is divided into the pre-chamber and the main chamber linked by a throat. In an IDI diesel engine, fuel injects into the pre-combustion chamber and air is pushed through the narrow passage on the compression stroke and becomes turbulent within the pre-chamber. This narrow passage speeds up the expanding gases more. The pre-chamber approximately contains 50% of the combustion volume when the piston is at TDC. This geometrical represents an additional difficulty to those deals with in the DI combustion chambers. Generally, IDI engines have lower performance than DI engines, because of their intense heat loss in swirl chamber throat [5].

Three dimensional modeling takes into account the interaction between different phenomena including

* Corresponding Author Email: S.Jafarmadar@Urmia.ac.ir (S. Jafarmadar)

turbulent flow, spray, combustion and naturally the geometry of combustion chamber. It allows a precise investigation of the problem as it provides all variable at all of the point. When applied to IDI engines, these models have to address specific problems linked to the flow unsteadiness, high Reynolds numbers involved, and the complex variable geometry of the solid boundaries. As a consequence, CFD calculations are usually take long solution time and also high computer memory is required, but these problems have been partially solved as a result of the significant improvement in power and speed of modern computers in recent years. In other words, simulation of the combustion system by means of computer modeling makes it possible to explore combustion regimes that may be difficult and/or expensive to achieve with experiments [6].

There are many experimental studies about using of alternative fuel, improving of combustion process and emission reduction in indirect injection diesel engines [7-11]. Yoshihiro Hotta and etc, progressed an experimental research for reducing the Particulate Matter (PM) from IDI diesel engine and examined the reducing mechanisms using an optically accessible engine at Toyota central research and development laboratories, Inc. [12].

In fact, it is now commonly admitted that the design of IDI combustion chambers has to rely increasingly more on fundamental knowledge of local aspect requiring multidimensional simulation. Many fundamental aspects concerning of CFD simulation of IDI engines have been discussed earlier by Pinchon [13].

Three dimensional modeling of combustion and soot formation in an indirect injection diesel engine using KIVA CFD code have been progressed by Zellat etc. [14]. Tim Sebastian and etc, at Volkswagen AG had studied the combustion and pollutant formation processes in a 1.9 l IDI diesel engine using SPEED CFD code for a part and full load. The global properties are presented resolved for the swirl and main chamber and the swirl chamber throat separately. The formation and thermal NOx and soot are simulated and analyzed as well [16].

As can be seen in the relevant literature, there are a few attempts about three dimensional modeling in IDI diesel engines up to now. At present work a CFD code has been used to predict and investigate the flow field, combustion process and emissions in the Lister 8.1 indirect injection diesel engine in full and part loads. Also performance parameters are calculated at the both load operations. Taking into account the rather complicated nature of the IDI diesel engine due to the continuous mass and energy exchange between the two chambers, we have decided to make an investigation on indirect injection diesel engine.

2. INITIAL AND BOUNDARY CONDITIONS

Calculations are carried out on the closed system from Intake Valve Closure (IVC) at 165°CA BTDC to Exhaust Valve Open (EVO) at 180°CA ATDC. Figures 1-a and 1-b show the numerical grid and its independence with a single hole injector mounted in pre-chamber, which is designed to model the geometry of the engine and contains a maximum of 42200 cells at 165°CA BTDC. The present resolution was found to give adequately grid independent results. Initial pressure in the combustion chamber is set to 86 kPa and initial temperature is calculated to be 384K, and swirl ratio is assumed to be on quiescent condition. Present work is studied for two loads: a full load and a part load (50% load) and for both cases the engine speed is 730 rev/min. All boundaries temperatures were assumed to be constant throughout the simulation, but allowed to vary with the combustion chamber surface regions.

3. MODEL FORMULATION

The numerical model is carried out for Lister 8.1 indirect injection diesel engine with the specification on Table 1. The governing equations for unsteady, compressible, turbulent reacting multi-component gas mixtures flow and thermal fields were solved from IVC to EVO by the commercial AVL-FIRE CFD code [16].

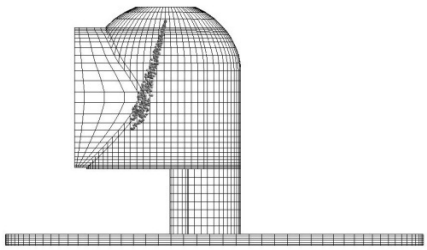

Figure 1-a. Mesh of the Lister 8.1 indirect injection diesel engine

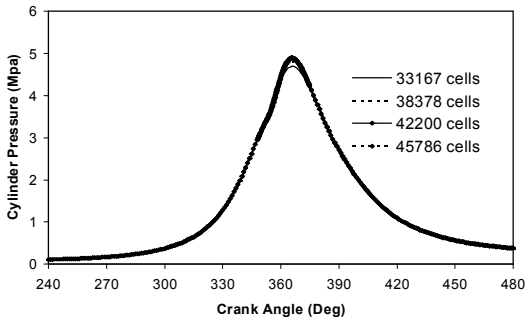

Figure 1-b. Grid dependency based on the in-cylinder pressure

The turbulent flows within the combustion chamber are simulated using the RNG $k-\varepsilon$ turbulence model, modified for variable-density engine flows [17]. The standard WAVE model, described in [18], is used for the primary and secondary atomization modeling of the resulting droplets. At this model the growth of an initial perturbation on a liquid surface is linked to its wave length and other physical and dynamical parameters of the injected fuel at the flow domain. Drop parcels are injected with characteristic size equal to the Nozzle exit diameter (blob injection). The injection rate profiles at the full and 50% load are shown in Figure 3.

The Dukowicz model is applied for treating the heat up and evaporation of the droplets, which is described in [19]. This model assumes a uniform droplet temperature. In addition, the droplet temperature change rate is determined by the heat balance, which states that the heat convection from the gas to the droplet either heats up the droplet or supplies heat for vaporization.

A Stochastic dispersion model was employed to take the effect of interaction between the particles and the turbulent eddies into account by adding a fluctuating velocity to the mean gas velocity [16]. This model assumes that the fluctuating velocity has a randomly Gaussian distribution.

The spray/wall interaction model used in this simulation was based on the spray/wall impingement model [20]. This model assumes that a droplet, which hits the wall is affected by rebound or reflection based on the Weber number. The Shell auto-ignition model was used for modeling of the auto ignition [21]. In this generic mechanism, 6 generic species for hydrocarbon fuel, oxidizer, total radical pool, branching agent, intermediate species and products were involved. In addition the important stages of auto ignition such as initiation, propagation, branching and termination were presented by generalized reactions, described in [16, 21].

The Eddy Break-up model (EBU) based on the turbulent mixing was used for modeling of the combustion process in the combustion chamber [16] as follows:

$$\overline{\rho \dot{r}_{fu}} = \frac{C_{fu}}{\tau_R} \bar{\rho} \min\left(\bar{y}_{fu}, \frac{\bar{y}_{ox}}{S}, \frac{C_{pr}.\bar{y}_{pr}}{1+S}\right) \quad (1)$$

where this model assumes that in premixed turbulent flames, the reactants (fuel and oxygen) are contained in the same eddies and are separated from eddies containing hot combustion products. The rate of dissipation of these eddies determines the rate of combustion. In other words, chemical reaction occurs fast and the combustion is mixing controlled .The first two terms of the "minimum value of" operator determine whether fuel or oxygen is present in limiting quantity, and the third term is a reaction probability which ensures that the flame is not spread in the absence of hot products. Above equation includes three constant coefficients (C_{fu}, τ_R, C_{pr}) and C_{fu} varies from 3 to 25 in diesel engines. An optimum value was selected according to experimental data [23]. NOx formation is modeled by the Zeldovich mechanism and Soot formation is modeled by Kennedy, Hiroyasu and Magnussen mechanism [22].

TABLE 1. Specifications of Lister 8.1 IDI diesel engine

Cycle Type	Four Stroke
Number of Cylinders	1
Injection Type	IDI
Cylinder Bore	114.1 mm
Stroke	139.7 mm
L/R	4
Displacement Volume	1.43 lit.
Compression Ratio	17.5 : 1
Vpre-chamber/VTDC	0.7
Full Load Injected Mass	$6.4336e-5$ kg per Cycle
Power on 850 rpm	5.9 kW
Power on 650 rpm	4.4 kW
Initial Injection Pressure	90 bar
Nozzle Diameter at Hole Center	0.003 m
Number of Nuzzle Holes	1
Nozzle Outer diameter	0.0003 m
Spray Cone Angle	10°
Valve Timing	IVO= 5° BTDC
	IVC= 15° ABDC
	EVO= 55° BBDC
	EVC= 15° ATDC

4. RESULTS AND DISCUSSION

The calculations of availability terms are carried out for the single cylinder Lister 8.1 IDI diesel engine and the operating conditions are full and 50% loads at constant speed 730 rev/min.

Figure 2 shows the verification of computed and measured [23] mean in-cylinder pressures for both cases. This figure shows that both computational and experimental pressures during the compression and expansion strokes are in excellent agreement. Comparing these figures also show the effect of load on in-cylinder pressure. The results which are presented in

these figures are global (cylinder averaged) quantities as a function of time (crank angle). Fuel injection timing and amount of injected mass were the changed parameters for loads and the remaining initial conditions were unchanged. The peak pressures discrepancy between experiment and computation are less than 0.2%. Increasing load to full load mode causes in-cylinder peak pressure increased to 50.2 bar from 42.3 bar and ignition delay decreased to 7.9 CAD from 10.7 CAD respect to 50% load. At full load operation because of fuel injecting in later cycle and also long injection duration, more fuel injected burns in diffusion phase. This figure also shows the quantity of computational and experimental start of combustion (SOC) and ignition delay (ID) degrees in both cases. The discrepancies of SOC or ID between computation and experiment at part load and full load operation are only 0.8° and 0.1° crank angle respectively. Figure 3 shows the development of the burnt mass fraction. We find a classical result as to the relation between the values for the main and the pre-chamber. As seen in these figures, the start of combustion is early at the full load than part load in the pre-chamber. Also it is observed that at the full load, computed burn fuel mass fraction and then heat release rate equality is shared between the main and the pre-chamber. The simulation correctly represents a typical feature at part load because of more fuel burning in main chamber.

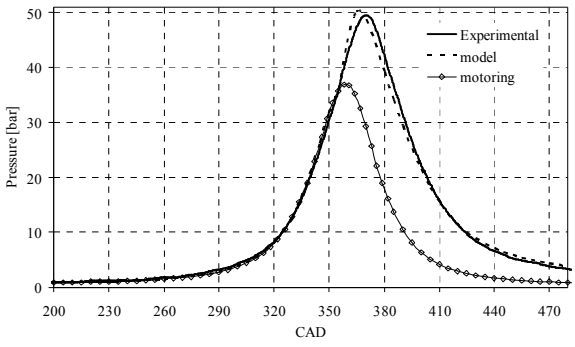

(a)

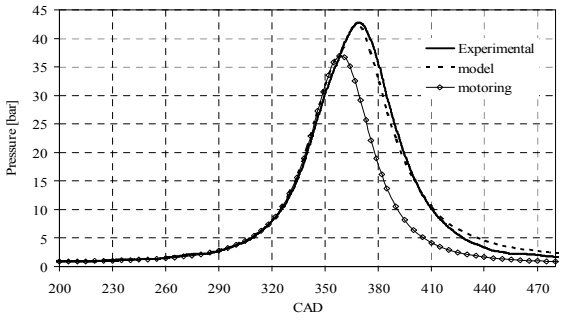

(b)

Figure 2. Comparison of measured [23] and calculated pressure at 730 rev/min for (a) full and (b) part load

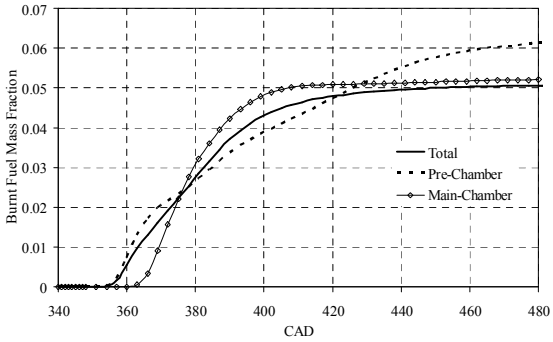

(a)

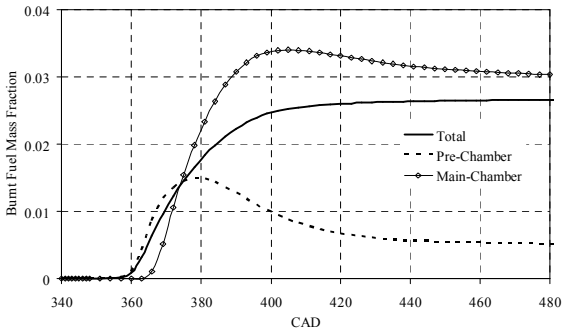

(b)

Figure 3. calculated burn fuel mass fraction at 730 rev/min for (a) full load and (b) part load.

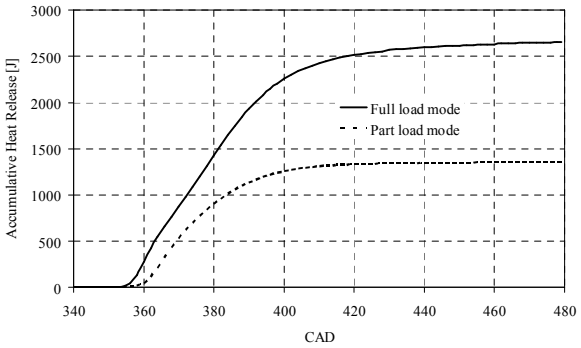

Figure 4. Accumulated heat release rate at 730 rev. /min for full and part load operations

Figure 4 indicates the accumulated heat release rate at full and part load operations. As shown in this figure, accumulated heat release rate at full operation is about 2 times higher that part load operation. Also, start of combustion in pre-chamber is earlier in full load than that of part load. At combustion duration, accumulative heat release rate increases due fuel burning and combustion process occurrence. Figure 5 indicates the heat loss rate in pre and main chambers at two loads. It is clear from this figure that the main part of heat loss takes place in pre-chamber, although the volume ratio of

pre-chamber to total volume at TDC is equal to 0.7. At part load, the amount of heat loss in pre and main chambers is the same, while at full load operation the amount of heat loss from pre-chamber is greater than that of main-chamber. The temperature histories are presented region-resolved for the swirl, main and total in-cylinder chamber in Figure 6. It shows that temperature peak values in the swirl chamber, main chamber and total are respectively 1394, 1612, and 1389 K at part load and they are respectively 1788, 1966, and 1827K for full load operation. When the engine load increases at constant speed (730 rev/min) from 50% load to full load, the peak temperature quantities in swirl, main and total in-cylinder chamber increase by 394, 354 and 438K respectively. The increase in load results an increase in the equivalence ratio since the amount of injected fuel increased in the constant air mass in the pre-chamber. This tends to increase the air temperatures and thus increases the chances of forming a flammable mixture for pre-flame reactions to take place. This reduces the ignition delay period in the pre-chamber. Also at the full load operation because of long injection duration, combustion period is longer than the part load operation. Therefore temperatures in the swirl, main and total in-cylinder chamber at full load are higher than their temperature at 50% load operation at the expansion stroke. Also at the indirect injection (IDI) diesel engine, since the fuel spray is injected into an auxiliary chamber such as a swirl chamber, most of the fuel spray stays in it especially at full load operation. Wall impinged fuel gradually evaporates and burns in it. Therefore combustion period in pre-chamber is long at full load operation (see Figure 4-a).

Figure 7 represent the evolution of the velocity field at various crank angles in horizontal planes of main combustion chamber and planes across the connecting throat. It can be seen that the maximum velocity at whole crank angles because of large area at throat section are lower than the others data in the literatures [5, 12-14]. The maximum velocity for full load operation is 56 m/s at 10 CA ATDC due to start of combustion in pre-chamber and the maximum mass flows out from it. Figure 7 also indicates that the swirl which is generated during the compression stroke (20 CA BTDC at Figure 7) became gradually weaker due to opposite flow in glow plug. At 60 CA ATDC velocities get dominated by the evacuation of pre-chamber. The flow in throat changes its direction at the beginning of combustion and after TDC the flow in the pre-chamber is strongly influenced by the fuel spray. It is observed the evolution of velocity field in the main chamber at the top and front view at this figure. From top view at 20 CA ATDC, we notice to the formation of two vortices that created by the decelerating the axial penetration of the mixture.

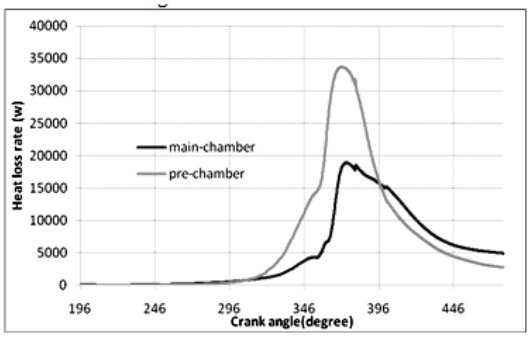

(a)

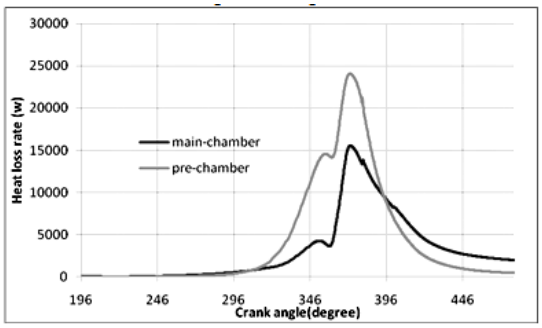

(b)

Figure 5. calculated rate of heat loss in pre and main-chambers at 730 rev/min for (a) full load and (b) part loads.

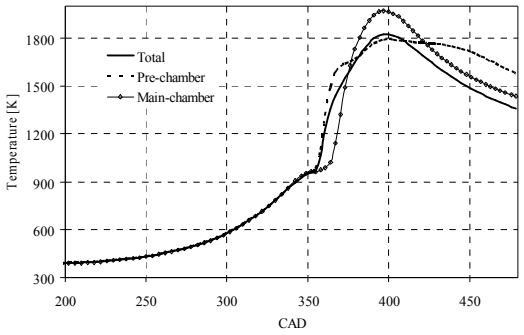

(a)

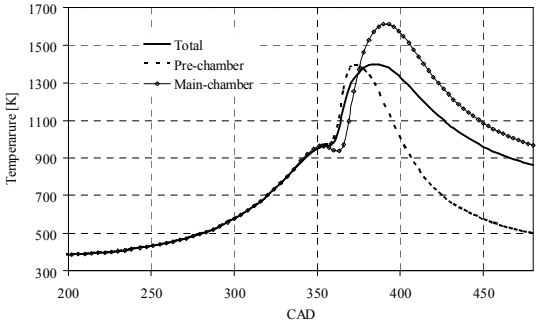

(b)

Figure 6. Comparison of experimental and calculated heat release rate at 730 rev/min for (a) full and (b) part loads

From front view at 40 CA ATDC, the gas coming from the pre-chamber reaches the opposite side of cylinder. This leads to the formation of two large eddies occupying each one half of the main chamber and staying centered with respect to the two half of the bowl. At 60 CA ATDC, these eddies are bigger. Flow field in part load operation is similar to full load, whereas that maximum velocity is 61m/s.

In Figure 8 the evolution of the fuel jet (spray) and vapor saturation are presented from start of injection at 10 CA BTDC to 35 CA ATDC. The velocity flow field shown in Figure 7 explains why the spray conserves initial direction imposed by the injector. As shown this figure, fuel vapor – air mixing in the pre-chamber because of vortex existence at the full load operation is better than the part load. Also Fuel spray impinges against the chamber wall from the beginning due to less interaction between flow field and spray. We observe that an increased engine load yields more vapors and more liquid in the pre-chamber at the beginning of combustion. This is probably at the origin of the much higher soot quantity presented in the pre-chamber in full load operation. The hard spray impingement causes fuel adhesion on the wall near spray-wall impinging point. This adherent fuel is not quickly evaporated and formed fuel vapor is hardly carried out of this area, because the stagnation zone is formed here due to the chamber shape. Thus it is possible; the rich fuel-air mixture stagnates in this zone under the condition of high temperature and insufficient oxygen to form the dense soot cloud. In the following, the production of NOx, soot and TUHC as main emissions in IDI diesel engines are discussed. Also NOx and TUHC exhaust values are verified with experiment for both cases. Results indicate that NOx emission has a good agreement with experiments in full load operation while at part load operation not is verified with experiment. At both loads, TUHC emission exactly can be predicted by model. As the fuel injection is delayed (retarded), the time available for air/fuel mixing and combustion is reduced, and, the consumption rate of the fuel decreases. The fuel consumption rate becomes much slower with very late injection, resulting in significant increases in the unburned fuel amount. Also at the present cases observe similar behaviors.

As shown in Figure 9, under high load conditions, the main cause of the exhaust smoke is both of the fuel adhesion to the chamber wall and the stagnation of rich fuel-air mixture. Also it can be seen that the area which the equivalence ratio is close to 1 and the temperature is higher than 2000 K is the NOx formation area. In addition, the area which the equivalence ratio is higher than 3 and the temperature is approximately between 1600 K and 2000 K is the Soot formation area. A local soot-NOx trade-off is evident in these contour plots, as the NOx and Soot formation occur on opposite sides of the high temperature region [24].

The temperature evolution reveals that the flame started in pre-chamber and invades very quickly a large part of the main-chamber. We observe the beginning of the mass transfer between pre-chamber and chamber around TDC. The development of the temperature field between 20 and 30 CA ATDC shows that the axial and the radial penetrations of the flame front are almost equal. Thus, the flame front reaches the lateral cylinder wall and the cylinder wall opposite to the pre-chamber at nearly the same lime. The fast decrease of the oxygen concentration in main and pre-chamber corresponds to a large zone of high temperature (over 2000 K at 10 CA ATDC).

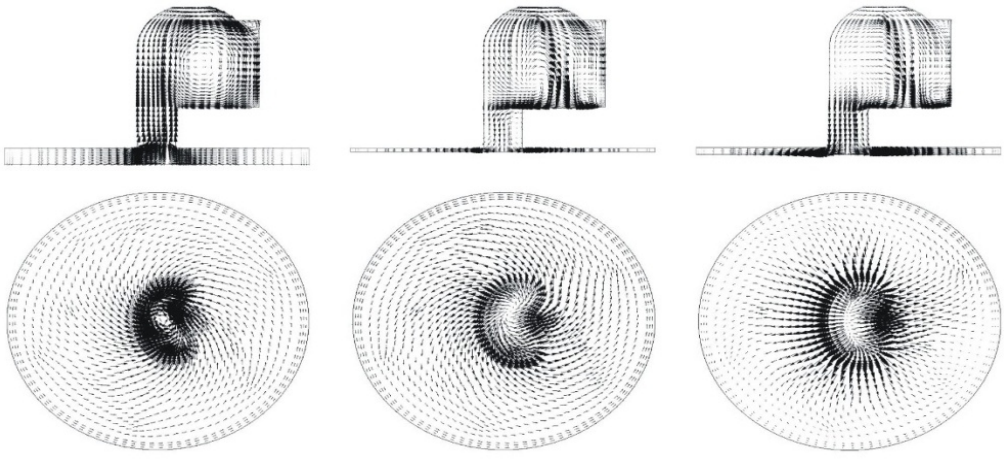

20 CAD BTDC, V_{max}= 47 m/s TDC, V_{max}= 48 m/s 10 CAD ATDC, V_{max}= 56 m/s

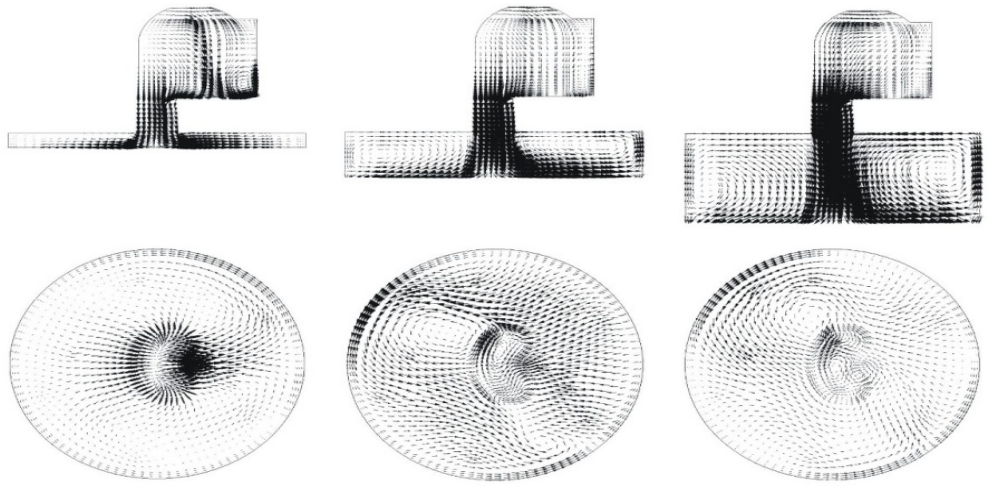

Figure 7. Velocity vector plots for full load operation

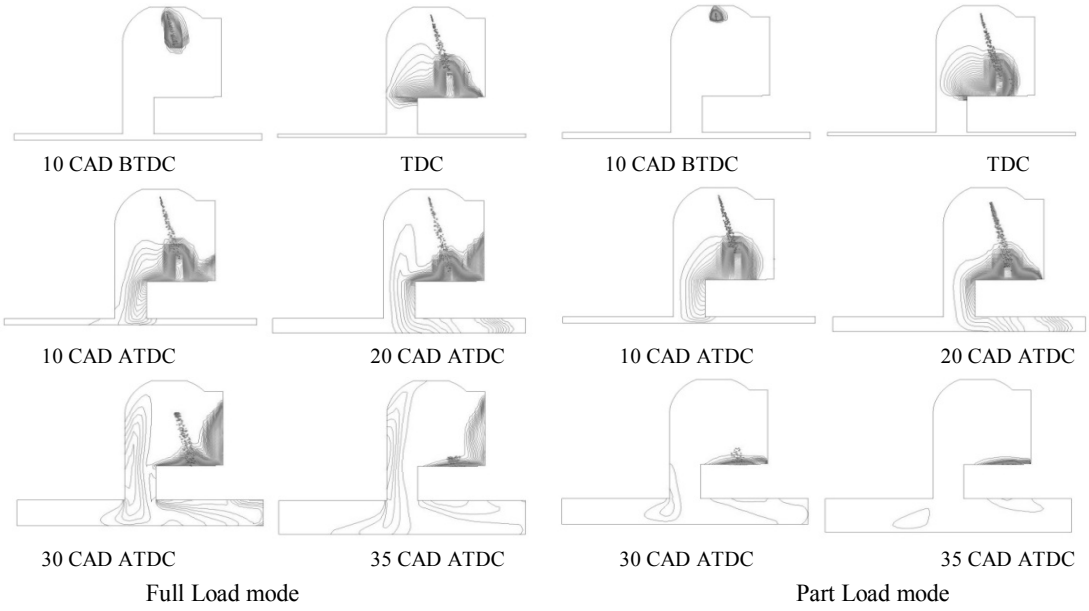

Figure 8. Spray and vapor saturation contours

The region resolved global mass fractions of NOx for the two cases are given in Figures 10-a and 10-b. NOx formation starts off at about 17CA and 18CA for full and part load operation after the start of injection respectively. The initial increase in the global NOx mass fractions follows the global temperature (see Figure 6). Also it is observed that NOx formation in main chamber is bigger than in pre-chamber especially in pat load operation. Finally in Figures 10-c and 10-d we present the evolution of the soot mass in the chamber and in the pre-chamber for the both loads. One notice that at part load, the maximum soot mass present in the main chamber is bigger than in the pre-chamber. However, soot combustion is so fast that the soot concentration of the exhaust gases is already attained at about 60 CA ATDC. In fact, because of the large quantity of oxygen available, the turbulent soot combustion diminishes the soot concentrations to 0.1gr/kw.hr at about 110 CA ATDC. At high loads, we observe that soot quantities in the pre-chamber is much bigger than main chamber due to stagnation region forming in glow plug and also shows that soot is

produced in regions of high fuel Concentrations, when cold fuel is injected into areas of hot gases. The soot then oxidizes again in the leaner Regions of the flame, so that close to the stocheometric zone most of the soot is already consumed. Soot quantities in the pre-chamber Vanishes due to soot combustion and convection to the main chamber due to the insufficient oxygen mass available.

In Figure 11, the production of UHC as main emissions in IDI diesel engines are discussed. Also UHC exhaust emission value is verified with experiment for both cases. Results indicate that UHC emission has a good agreement with experiments in full load operation while at part load operation not is verified with experiment. At both loads, TUHC emission exactly can be predicted by model. As the fuel injection is delayed (retarded), the time available for air/fuel mixing and combustion is reduced, and, the consumption rate of the fuel decreases. The fuel consumption rate becomes much slower with very late injection, resulting in significant increases in the unburned fuel amount

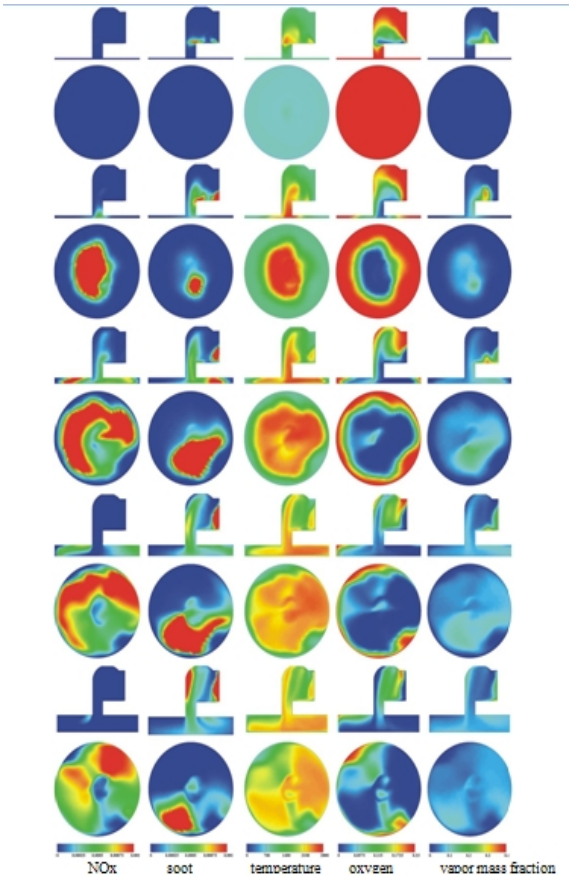

Figure 9. $NO_{x,}$, Soot ,temperature ,Oxygen and vapor mass fractions contour plots at full load operation(from left to right) for TDC,10,20,30,40 CA ATDC(from top to bottom)

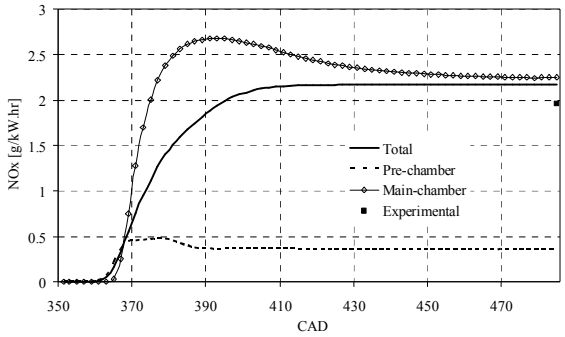

(a) Full load NOx

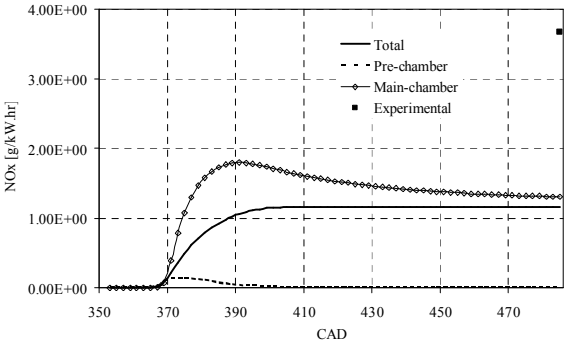

(b) Part load NOx

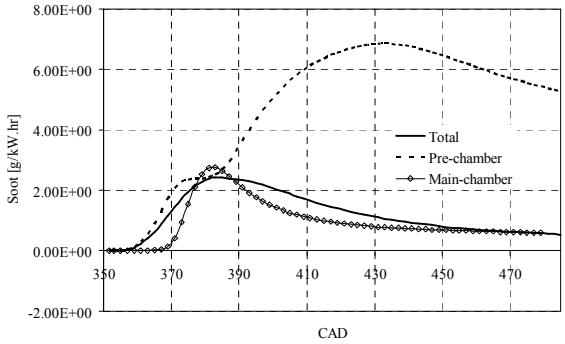

(c) Full load soot

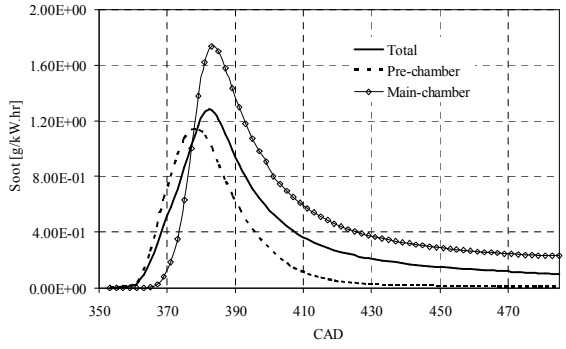

(d) Part load soot

Figure 10. Comparison of measured [23] and calculated exhaust emission at 730 rev/min for full and part load operation.

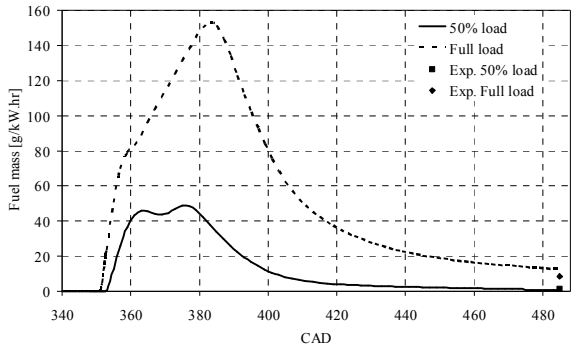

Figure 11. Comparison of measured [23] and calculated UHC exhaust emission at 730 rev/min for full and part load operation

5. CONCLUSION

The mixture formation, combustion processes, pollutant formation in pre and main chambers within Lister 8.1 IDI diesel engine have been studied for full and part load operations. The global properties are presented resolved for the swirl and main chamber separately. The result show that in the case of full load operation the amounts of burn fuel mass fraction and soot emission in pre chamber is higher than that of main chamber, while a large amount of NOx emission is produced in main chamber at both loads. As for the interpretation of the results, it can be seen a weak deflection of the fuel jet because of the low swirl level in the pre-chamber due to the presence of the glow plug. Results for calculated pressure, exhaust emissions and performance parameters are compared with the corresponding experimental data and show good agreement. Such verification between the experimental and computed results gives confidence in the model prediction, and suggests that the model may be used future works. The CFD simulations been shown to greatly improve the understanding and to facilitate the analysis of the combustion and pollutant formation processes in multi chamber diesel engines.

6. REFERENCES

1. Heywood. B., "Internal combustion engine fundamental" McGraw Hill Book Company, New York, (1988).
2. Benson R.S. and Whitehouse N.D. "Internal combustion engines", Pergamon Press, Oxford, (1979).
3. Ferguson C.R. "Internal combustion engines", John Wiley, New York, (1986).
4. Obert, E. F., "Internal combustion engines and air pollution", Intext Educ. Publ., New York, (1993).
5. Patterson, D. J and Henein, N. A., "Emissions from combustion engines and their control", Science Publ.,Michigan, (1972).
6. Uludogan A., Foster D. E., and Reitz, R. D., "Modeling the effect of engine Speed on the combustion process and emissions in a DI diesel engine", SAE paper 962056.
7. Sanli, A. , Ozsezen, A. N., Kilicaslan, I., Canakci, M., "The influence of engine speed and load on the heat transfer between gases and in-cylinder walls at fired and motored conditions of an IDI diesel engine", ***Applied Thermal Engineering*** , Vol. 28, (2008), 1395–1404.
8. Canakci, M., Ozsezen, A. N., Turkcan, A., "Combustion analysis of preheated crude sunflower oil in an IDI diesel engine", ***Biomass and Bioenergy*** , Vol. 33, (2009), 760 – 767.
9. Selim, M.Y.E., Radwan, M.S., Elfeky, S.M.S., "Combustion of jojoba methyl ester in an indirect injection diesel engine", ***Renewable Energy*** , Vol. 28, (2003), 1401–1420.
10. Celıkten, I., "An experimental investigation of the effect of the injection pressure on engine performance and exhaust emission in indirect injection diesel engines", ***Applied Thermal Engineering,*** Vol. 23, (2003), 2051–2060.
11. Parlak, A., Yasar, H., Hasimoglu, C., Kolip, A., "The effects of injection timing on NOx emissions of a low heat rejection indirect diesel injection engine", ***Applied Thermal Engineering*** , Vol. 25, (2005), 3042–3052.
12. Hotta,Y., Nakakita, K. and Inayoshi, M., "Combustion improvement for reducing exhaust emissions in IDI diesel engine", SAE 980503.
13. Pinchon, P. "Three dimensional modeling of combustion in a pre-chamber Diesel engine", SAE 890666.
14. Zellat M., Rolland Th. and Poplow F. "Three dimensional modeling of combustion and soot formation in an indirect injection diesel engine"; SAE 900254.
15. Tim Sebastian Strauss, George Wolfgang Schweimer. Combustion in a swirl chamber diesel engine simulation by computation of fluid dynamics. SAE 950280.
16. AVL FIRE user manual V. 8.5; (2006).
17. Han, Z., Reitz, R. D., "Turbulence Modeling of Internal Combustion Engines Using RNG K-e Models", ***Combustion Science and Technology,*** Vol. 106, (1995), 267-295.
18. Liu, AB, Reitz RD., "Modeling the effects of drop drag and break-up on fuel sprays", SAE, (1993), Paper NO. 930072.
19. Dukowicz, JK., "Quasi-steady droplet change in the presence of convection", Informal report Los Alamos Scientific Laboratory, LA7997-MS.
20. Naber, JD, Reitz RD., "Modeling engine spray/wall impingement", SAE, (1988), Paper NO. 880107.
21. Halstead, M., Kirsch, L., Quinn, C., "The Auto ignition of hydrocarbon fueled at high temperatures and pressures - fitting of a mathematical model", ***Combustion Flame***, Vol. 30, (1977), 45-60.
22. Patterson, M. A., Kong, S. C., Hampson, G. J., Reitz, R. D., "Modeling the Effects of Fuel Injection Characteristics on Diesel Engine Soot and NOx Emissions", SAE, (1994), Paper 940523,.
23. Mohammahi Kusha, A., "Ignition of dual fuel engines by using free radicals existing in EGR gases", PhD thesis. Faculty of mechanical engineering, Tabriz university, Iran (2008).
24. Carsten Baumgarten, "Mixture formation in internal combustion engines", Springer publications (2006).

Three Dimensional Modeling of Combustion Process and Emissions Formationin Pre and Main Chambers of an Idirect Injection Diesel Enginge

S. Jafarmadar, R. Barzegar

Department of Mechanical Engineering, University of Urmia, Urmia, Iran,

P A P E R I N F O

Paper history:
Received 16 May 2012
Received in revised form 10 July 2012
Accepted 30 August 2012

Keywords:
Main and Pre Chambers
Indirect Injection
Emission
Performance
Three Dimensional Modeling

چکیده

فرآیند احتراق و تشکیل آلاینده ها در داخل محفظه های اصلی و فرعی موتور لیستر ۸,۱ پاشش غیر مستقیم با استفاده از مدلسازی سه بعدی مطالعه شده است. مدل شامل اتمیزاسیون جت سوخت ، اماده سازی مخلوط و توزیع سوخت بوده و نهایتا مطالعه فرایند احتراق و تشکیل الاینده با در نظر گرفتن اثرات میدان جریان در دو محفظه انجام گرفته است.شبیه سازی در دوحالت بار ۵۰٪ و بار کامل انجام گرفته است. اندازه سوخت محترق شده، توریع دما، اتلافات حرارتی وتشکیل آلاینده ها در دو محفظه با جزئیات بیشتر ارائه شده است. نتایج برای فشار داخل سیلندر برای دو حالت با نتایج تجربی مقایسه شده و توافق خوبی نشان می دهند.نتایج ارائه شده در این کار نشان می دهند که مدلسازهای سه بعدی می تواند برای مدلسازی هندسه های پیچیده استفاده شده و برای دید بیشتر در مورد مطالعه میدان جریان ، فرایند احتراق و تشکیل آلاینده ها بکار گرفته شوند. نتایج عددی نشان می‌دهند که مدلسازی سه بعدی فرآیند احتراق و آلایندگی یک ابزار مناسب برای پیش گوئی فرآیند احتراق و آلایندگی محفظه های اصلی و فرعی موتور لیستر ۸,۱ پاشش می باشد

doi: *10.5829/idosi.ije.2012.25.04c.06*